

Unclassified  
SECURITY CLASSIFICATION OF T



## REPORT DOCUMENTATION PAGE

Form Approved  
OMB No. 0704-0188

1a. REPORT SECURITY CLASSIFICATION <b>Unclassified</b>		1b. RESTRICTIVE MARKINGS	
2a. SECURITY CLASSIFICATION AUTHORITY <b>DTIC ELECTE</b>		3. DISTRIBUTION/AVAILABILITY OF REPORT Approved for public release; Distribution unlimited	
2b. DECLASSIFICATION/DOWNGRADING SCHEDULE <b>MAY 23 1991</b>		4 PERFORMING ORGANIZATION REPORT NUMBER <b>PL-TR-91-2101</b>	
6a. NAME OF PERFORMING ORGANIZATION <b>Phillips Laboratory</b>		5 MONITORING ORGANIZATION REPORT NUMBER(S) <b>DTIC TAB</b> <input checked="" type="checkbox"/> <b>TRAVEL</b> <input type="checkbox"/>	
6b. OFFICE SYMBOL (If applicable) <b>PHK</b>		7a. NAME OF MONITORING ORGANIZATION <b>Justification</b>	
6c. ADDRESS (City, State, and ZIP Code) <b>Hanscom AFB Massachusetts 01731-5000</b>		7b. ADDRESS (City, State, and ZIP Code)	
8a. NAME OF FUNDING/SPONSORING ORGANIZATION		9 PROCUREMENT INSTRUMENT IDENTIFICATION NUMBER/ or <b>Dist Special</b> <b>A-1 20</b>	
8b. OFFICE SYMBOL (If applicable)		8c. ADDRESS (City, State, and ZIP Code)	
10 SOURCE OF FUNDING NUMBERS			
PROGRAM ELEMENT NO <b>62101F</b>	PROJECT NO. <b>7601</b>	TASK NO. <b>30</b>	WORK UNIT ACCESSION NO. <b>06</b>
11. TITLE (Include Security Classification) <b>Current Saturation of Electron Beam Emission from the SCATHA Satellite</b>			
12. PERSONAL AUTHOR(S) <b>S.T. Lai</b>			
13a. TYPE OF REPORT <b>Reprint</b>	13b. TIME COVERED FROM _____ TO _____	14. DATE OF REPORT (Year, Month, Day) <b>1991 May 6</b>	15. PAGE COUNT <b>9</b>
16 SUPPLEMENTARY NOTATION <b>Reprinted from Proceedings of the Spacecraft Charging Technology Conference, Naval Postgraduate School, Monterey, CA 31 Oct - 3 Nov 1989</b>			
17. COSATI CODES		18. SUBJECT TERMS (Continue on reverse if necessary and identify by block number)	
FIELD	GROUP	SUB-GROUP	Spacecraft charging, Electron beam, Geosynchronous, SCATHA, Booms
19. ABSTRACT (Continue on reverse if necessary and identify by block number)			
<p style="text-align: center;">Data taken from SCATHA show that when the satellite is charged to near electron beam energy, saturation behavior in the current-voltage curve occurs. We analyse SC10 data of boom-satellite potential difference to obtain the satellite potential as a function of electron beam current emitted. As the satellite rotates in sunlight, a fraction of the photoelectron current generated on the long booms is received by the satellite body. The satellite potential is governed by the balance of currents of outgoing electron beam, incoming photoelectrons, and ambient plasma. The SC10 data are modulated at a frequency of twice per satellite rotation in sunlight. By means of a simple model of partial return of photoelectrons and beam electrons, we explain the saturation behavior of the modulating SC10 data obtained during high current electron beam emissions resulting in the charging of the satellite to near beam potential. The returning electron beam current as a function of emitted beam current is deduced.</p>			
20. DISTRIBUTION/AVAILABILITY OF ABSTRACT <input type="checkbox"/> UNCLASSIFIED/UNLIMITED <input checked="" type="checkbox"/> SAME AS RPT. <input type="checkbox"/> DTIC USERS		21. ABSTRACT SECURITY CLASSIFICATION <b>Unclassified</b>	
22a. NAME OF RESPONSIBLE INDIVIDUAL <b>S.T. Lai</b>		22b. TELEPHONE (Include Area Code) <b>(617) 377-2932</b>	22c. OFFICE SYMBOL <b>PHK</b>

DTIC  
UNCLASSIFIED

2

## Current Saturation of Electron Beam Emission from the SCATHA Satellite

S.T. Lai

Geophysics Laboratory, Hanscom AFB, 01731

 DTIC  
 ELECTE  
 MAY 23 1991  
 S C D

## ABSTRACT

Data taken from SCATHA show that when the satellite is charged to near electron beam energy, saturation behavior in the current-voltage curve occurs. We analyse SC10 data of boom-satellite potential difference to obtain the satellite potential as a function of electron beam current emitted. As the satellite rotates in sunlight, a fraction of the photoelectron current generated on the long booms is received by the satellite body. The satellite potential is governed by the balance of currents of outgoing electron beam, incoming photoelectrons, and ambient plasma. The SC10 data are modulated at a frequency of twice per satellite rotation in sunlight. By means of a simple model of partial return of photoelectrons and beam electrons, we explain the saturation behavior of the modulating SC10 data obtained during high current electron beam emissions resulting in the charging of the satellite to near beam potential. The returning electron beam current as a function of emitted beam current is deduced.

## INTRODUCTION

The SCATHA satellite was launched in 1979 for investigating problems of spacecraft charging at geosynchronous altitudes. Descriptions of the experiments on board SCATHA have been given by *Stevens and Vampola* [1978] and *Fennell* [1982]. The satellite, about 1m long and 1.6m in diameter, spins at about once per 60s, and is equipped with two 50m booms (SC10) deployed oppositely in the equatorial plane (Figure 1). The SC10 booms are electrically isolated from the satellite. The outer 20m of each boom is a copper beryllium (CuBe) alloy. The inner segment is coated with Kapton, an insulating material. The SC10 data  $\phi$  represent the difference between the potential  $\phi_{\text{CuBe}}$  of the tip of a boom and that  $\phi_s$  of the satellite body (ground) [Aggson *et al*, 1983]. That is

$$\phi = \phi_{\text{CuBe}} - \phi_s \quad (1)$$

An electron beam (SC4-1) can be emitted from SCATHA with various energies and currents. During quiet days, the satellite is normally charged positively to a few Volts in sunlight. The emission of an electron beam tends to raise the satellite potential, depending on the ambient condition, beam energies and currents. When the satellite is rotating in sunlight, the amount of sunlight received by boom surfaces vary sinusoidally, and therefore the photoelectron current from the booms varies likewise.

When the satellite body is charged positively as a result of electron beam emission, there is a tendency for the photoelectrons from the booms to be attracted by the satellite body [Lai *et al*, 1987]. The booms form part of the satellite body's environment. In this case, the satellite body not only interacts with its ambient plasma environment but also with the booms which are electrically isolated from the body. This is a case of *Multi-body Interaction* in spacecraft charging.

Electron current saturation in diode tubes is well known [Child, 1911; Langmuir, 1912]. In a diode tube, the distance and potential difference between the electrodes are controlled parameters. As the current density increases, so does the space charge. Beyond a critical current density, the

91 5 22 008<sup>455</sup>91-00275  


space charge tends to return part of the current; only a fraction of the emitted current arrives at the anode. This is known as current saturation. The space charge limiting current is given by the famous *three-halves power law* [Child, 1911; Langmuir, 1912].

In space, however, the situation of an electron beam is different from that in a diode. The distance between the cathode and the anode in space is ill-defined, because, unlike a diode, it is not clear where the anode is in space. Furthermore, the beam emitted into space is not well collimated because the beam space charge tends to make the beam divergent. Therefore, it is interesting to ask whether current limitation can occur in beams emitted into space, and, if it does, whether there is a critical current under given experimental conditions.

Observations of current limitation in beam experiments on satellites have been reported. Olsen [1985] has presented ATS-5 results. Lai et al [1987] have presented SCATHA Day 89 results. The Day 89 data span a wide range of beam currents and energies and the data points are widely separated. To follow the development of current saturation and to pin point the sudden appearance of a critical current, it is necessary to choose a day in which the beam current increases continuously.

In the following sections, we will briefly discuss SCATHA SC10 data taken on Day 89, 1979. A theoretical model of photoelectron current modulation during electron beam emissions is presented. The SC10 data of Day 70 are particularly interesting because they feature a continuous increase in electron beam current while the beam energy is held constant and the environment is quiet. This gives a rare opportunity to observe spacecraft charging in response to a known driving factor: the beam current. The purpose in this case study is to compare theoretical and experimental results and to determine the critical current for the onset of current limitation.

### SCATHA CHARGING DURING ELECTRON BEAM EMISSIONS

Due to the high secondary emission coefficient of CuBe, the outer section of a SC10 boom is not expected to be charged to high potentials, except in unusually energetic ambient conditions. When the potential  $\phi_s$  is high compared with  $\phi_{\text{CuBe}}$ , the SC10 data  $\phi$  represents a good approximation of  $\phi_s$  with the sign reversed. There are other instruments measuring spacecraft potential on SCATHA. They show that SC10 data often give good approximate measurements of the satellite potential. We will assume that SC10 data  $\phi$  is  $-\phi_s$  approximately, since we consider quiet days only.

When SCATHA is in sunlight, with or without beam emission, SC10 data show oscillations at twice the satellite rotation frequency [Lai et al, 1986, 1987]. When the satellite is entering eclipse, the amplitude of oscillation decreases gradually [Cohen et al, 1981]; this evidence supports the contention that the oscillation is due to the effects of photoelectrons.

In total eclipse, SC10 data still show some insignificant but noticeable oscillation with a small amplitude, which, with its low signal to noise ratio, correlates weakly with the boom sun angle. The reason of this barely noticeable oscillation in eclipse is unknown. Some plausible reasons are (1) the sun in UV is bigger than what it appears to be, (2) there is a weak ambient magnetic field effect, or (3) there are anisotropic ambient currents. This property, however, is outside the scope of this paper.

In sunlight without electron beam emission, several aspects of SC10 data resemble those with electron beam emission. Sinusoidal oscillations are present, with the same frequency and boom sun angle correlation. The amplitude of oscillation is about 4 to 5 volts typically on quiet days [Lai et al, 1986].

As the electron beam current increases from zero, the spacecraft potential increases. And, not only the magnitude of SC10 data but also that of the oscillation increases. The extrema of the oscillation correlate well with the sun angle of the booms [Lai et al, 1987]. The minima occur at  $\theta=0^\circ$  and  $\theta=180^\circ$  and the maxima at  $90^\circ$  and  $270^\circ$ . Another instrument, SC2, also measures the potential of the spacecraft body. The oscillation frequency and phase of SC2 data are identical with those of SC10; this evidence shows that the oscillations are due to the variations of the potential of the spacecraft body.

The amplitude  $\Delta\phi$  of the SC10 data variation is a function of beam current and beam energy. The ratio of amplitude  $\Delta\phi$  to the satellite potential  $\theta$  shows nonmonotonic behavior as a function of beam current. The ratio first increases with the beam current until a maximum is reached and then it decreases as beam current further increases. When the beam current is large, the satellite is

charged to near beam energy, while the variations almost cease. Our contention is that, at large beam currents, the beam does not leave completely because of some current limiting mechanism, a saturation behavior.

Despite the wide range of combinations of beam current and energy on Day 89, 1979, the data are widely separated. In order to show the response of the satellite potential  $\phi_s$  to continuously increase in beam current, we present the Day 70, 1981 data (Figure 2). The beam energy is controlled at 300 eV constantly. The electron beam current increases continuously from near zero to about 90  $\mu$ A. There are several 30sec periods of dropouts (for calibration purposes) at regular intervals; the data in these periods are ignored in our study. The oscillation in the Day 70 data correlates with boom sun angle  $\theta$  in the same manner as in Day 89, the maxima of spacecraft potential occur when the booms are parallel or antiparallel to sunlight, and minima occur when the booms are perpendicular to sunlight. Starting from zero current, the oscillation amplitude increases monotonically with beam current until a critical current (about 60  $\mu$ A) is reached; then it decreases slightly with further increase in beam current. Unlike the Day 89 data, the continuous nature of the increasing beam current enables the critical current to be determined with better accuracy.

### THEORY OF PHOTOELECTRON CURRENT MODULATION

The photoelectron current from the booms depends on the sun angle  $\theta$ . Depending on the potential  $\phi_s$  of the satellite body, a fraction  $f$  of this current is received by the body. In a self-consistent manner, the satellite potential  $\phi_s$  depends on the photoelectron current  $I_{ph}$  received. In the low density plasma environment at geosynchronous altitudes, the orbit-limiting Langmuir plasma probe model is applicable for the collection of ambient current. The current balance equation for the satellite body is

$$I_e(0)(1+e\phi_s/kT_e)^\alpha + I_{ph}(\phi) = I_{beam}(\phi) - I_{return}(\phi) \quad (2)$$

and

$$I_{ph}(\phi) = 2d \int_0^{50m} dr f[\phi(r)] j_{ph} \sin \theta \quad (3)$$

where  $I_e(0)$  is the ambient current collected if the spacecraft potential  $\phi_s$  is zero without photoelectron or beam emission.  $I_{beam}$  is the electron beam current emitted. If the beam energy is high and the beam current density low, the whole beam leaves. However, if the beam energy is low and the beam current density is high, part of the beam may return and the return current  $I_{return}$  becomes nonzero. For a spherical body, the power  $\alpha$  of the orbit-limiting current collection term in eq(1) equals unity; for an infinite cylinder,  $\alpha$  equals 1/2. However, for SCATHA, the geometry of the satellite body resembles a sphere more than a cylinder. Thus, the power  $\alpha$  of the Langmuir orbit-limiting current collection term for SCATHA should be near unity; the exact value of  $\alpha$  is not needed for our purposes in this paper. The photoemissivity of the copper beryllium boom surface material on a rotating satellite (at about 1 AU) has been estimated to be  $2 \times 10^{-9}$  to  $4 \times 10^{-9}$  amp.cm<sup>-2</sup> [Kellogg, 1980]. The photoemissivity  $j_{ph}$  of the CuBe surfaces on the SC10 booms of SCATHA is considered as a parameter to be determined in this paper.

To model  $I_{ph}(\phi)$ , it is necessary to assume a photoelectron energy spectrum and a satellite sheath potential profile. Both laboratory and space experiments have shown that a Maxwellian distribution is a good approximation to describe the photoelectron energy spectrum [Hinteregger et al, 1965; Whipple, 1982]. Our model assumes energy partition of the spectrum.

$$f[\phi(r)] = \frac{\int_0^{e\phi(r)} dE E \exp(-E/kT_{ph})}{\int_0^\infty dE E \exp(-E/kT_{ph})} \quad (4)$$

where the satellite sheath potential  $\phi(r)$  is often modeled by the Debye form [Godard and Laframboise, 1973].

$$\phi(r) = \frac{\phi_s R}{r + R} \exp(-r / \lambda_D) \quad (5)$$

The Debye length  $\lambda_D$  of the ambient plasma is about 45m [Aggson, *et al*, 1983]. The photoelectron temperature  $T_{ph}$  is about 2 eV [Whipple, 1982; Lai *et al*, 1986]. Using this model, we compute the total photoelectron current going towards the satellite body (Figure 3).

The maxima and minima of the SC10 data of Figure 2 are plotted in Figure 4 as emitted beam current versus satellite potential. The data with photoemission (minimum  $|\phi|$  with  $\theta=90^\circ$  or  $270^\circ$ ) are plotted in Figure 5, and those without photoemission (maximum  $|\phi|$  with  $\theta=0$  or  $180^\circ$ ) in Figure 6. At low beam currents, each set of data follows a smooth trend. Each trend deviates suddenly at a critical current. Without photoemission, the critical current is about 60  $\mu A$  with the spacecraft potential at about 220 Volt. With photoemission, the critical current is higher (about 70  $\mu A$ ) with the spacecraft at a lower potential (about 140 Volt). Using the maximum  $|\phi|$  ( $\theta=0$  or  $180^\circ$ ) data curve (without photoelectrons), the total photoelectron current  $I_{ph}(\phi)$  is computed for a given photoemissivity  $j_{ph}$ . The total photoelectron current  $I_{ph}$  is then added to the maximum  $|\phi|$  ( $\theta=0$  or  $180^\circ$ ) curve. The theoretical curve obtained fits fairly well with the experimental data points of minimum  $|\phi|$  (with  $\theta=90^\circ$  or  $270^\circ$ ). We determine that the photoemissivity  $j_{ph}$  of the CuBe surfaces on the SC10 booms of SCATHA is about 3 nanoamp.cm<sup>-2</sup>, which agrees with the values (2 to 4 nanoamp.cm<sup>-2</sup>) estimated by Kellogg [1980] for the CuBe surfaces on a different spacecraft (Helios at 1 AU).

The satellite potential  $\phi_s(\theta)$  oscillates as the satellite and booms rotate in sunlight. The amplitude of potential oscillation is given by  $\Delta\phi = \phi_s(\theta=0 \text{ or } 180^\circ) - \phi_s(\theta=90^\circ \text{ or } 270^\circ)$ . As the beam current  $I_{beam}$  increases, so does the potential oscillation amplitude  $\Delta\phi$ . When the satellite is charged to near beam potential, the beam current ceases to leave completely. A non-monotonic behavior of the SC10 oscillation amplitude  $\Delta\phi$  ensues [Figure 7].

## ELECTRON BEAM SATURATION

When the beam current is saturated, the beam current leaving is less than the beam current emitted. Part of the beam returns (i.e.  $I_{return} \geq 0$ ). When saturation occurs, the data points on the current-voltage curves (Figures 5,6) deviate from the smooth trend set by the unsaturated points. Physically, when saturation occurs, the net current leaving the system is less than the emitted beam current. Mathematically, when saturation occurs, the net current  $I_{net} = I_{beam} - I_{return}$  (eq.2) should be used as the ordinate variable in place of  $I_{beam}$ . If  $I_{net}$  is used, the data points should again satisfy the same function, or curve, extrapolated from the unsaturated regime. Conversely, if the data points satisfy the extrapolated function, then the net current  $I_{net}$ , and hence the return current  $I_{return}$ , can be determined. Thus, this method allows one to determine the magnitude of return current  $I_{return}$  during beam saturation. The return current  $I_{return}$  are shown in Figures 5 and 6.

Also shown in Figure 5 and 6 are three regimes I, II, and III. In regime I and II, the beam current  $I_{beam}$  is unsaturated, and the return current  $I_{return}$  is zero. In regime I, photoelectron current from the satellite body can leave because the satellite positive potential  $\phi_s$  is low. The amount of photoelectron current leaving is a function of satellite potential  $\phi_s$ . An extrapolation of the regime II curve intercepts the y-axis (zero  $\phi_s$ ) at about 10  $\mu A$  (Figure 5); this determines the  $I_e(0)$  term in eq(2). Using the typical ambient current [Purvis *et al*, 1984] at geosynchronous altitudes on quiet days and the dimension of SCATHA, one obtains a result of the same order of magnitude for  $I_e(0)$ , the ambient current intercepted by SCATHA. With photoelectrons leaving the spacecraft body, the data points in regime I deviate from the curve extrapolated from regime II. With an estimated photoelectron current of about 30  $\mu A$  (which depends on the photoemissivity of the surface materials) leaving the spacecraft body at  $\phi_s=0$ , the data points (circles) are expected to intercept the y-axis at  $I_e(0)-30 \mu A$ , i.e. at  $-20 \mu A$ . In regime I, very little of the photoelectron current from the booms can reach the spacecraft body because of the low attraction offered by the low spacecraft potential  $\phi_s$ . In regime II, the multi-body interaction between the satellite body, the booms, the

electron beam, and the ambient plasma is in action. In regime III, beam saturation occurs and part of the beam current returns. Schematically, the physical processes in the three regimes are shown at the bottoms of Figure 5 and 6.

The details of the physical mechanism leading to the electron beam saturation are not known at this time. Space charge limitation [Lai et al, 1980], beam energy broadening [Katz, et al, 1986] and spacecraft differential charging [Olsen, 1985] are plausible mechanisms to be studied. The results of this study may be useful for obtaining new insights into beam saturation mechanisms in space.

#### REFERENCES

- Aggson, T.L., B.G. Ledley, A. Egeland, and I. Katz, Probe measurements of DC electric fields, *ESA-SP-198*, pp.13-17, 1983.
- Cohen, H.A., et al, P78-2 satellite and payload responses to electron beam operations on March 20, 1979, *NASA CP-2182*, 1981.
- Fennell, J.F., Description of P78-2 (SCATHA) satellite and experiments, in *IMS Source Book*, Am. Geophys. U., Washington, D.C. 1982.
- Godard, R. and J.G. Laframboise, A symmetrical model for the current collection of a spherical electrostatic probe in a flowing plasma, *EOS*, 54, 392, 1973.
- Hinteregger, H.E., L.A. Hall, and G. Schmidtke, Solar XUV radiation and neutral particle distribution in July 1963 thermosphere, *Space Physics*, Vol.5, 1175, 1965.
- Katz, I., G.A. Joneward, D.E. Parks, D.L. Reasoner and C.K. Purvis, Energy broadening due to spacecharge oscillations in high current electron beams, *Geophys. Res. Lett.*, Vol.13, 64, 1986.
- Kellogg, P.J., Measurements of potential of a cylindrical monopole antenna on a rotating satellite, *J. Geophys. Res.*, A85, 5157, 1980.
- Lai, S.T. and H.A. Cohen, Space charge in electron and ion beams emitted from P78-2 satellite, *EOS*, Vol.61, No.17, p.1090, 1980.
- Lai S.T., H.A. Cohen, T.L. Aggson, W.J. McNeil, Boom potential on a rotating satellite in sunlight, *J. Geophys. Res.*, Vol.91, No.A11, pp.12137-12141, Oct., 1986.
- Lai S.T., H.A. Cohen, T.L. Aggson, W.J. McNeil, The effect of photoelectrons on boom-satellite potential differences during electron beam ejections, *J. Geophys. Res.*, Vol.92, No.A11, pp.12319-12325, 1987.
- Langmuir, I., The effect of space charge and residual gases on thermionic currents in high vacuum, *Phys. Rev.*, Vol.2, 450, 1913.
- Olsen, R.C., Experiments in charge control of geosynchronous orbit - AT5 and AT6, *J. Spacecraft & Rockets*, Vol.22, pp.254-264, 1985.
- Purvis, C.K., H.B. Garrett, A.C. Whittlesey, and N.J. Stevens, Design guidelines for assessing and controlling spacecraft charging effects, *Rep. NASA-TP-2361, N84-33452*, 44pp., 1984.
- Stevens, J.R., and A.L. Vampola (Eds), Description of the space test program P78-2 spacecraft and payloads, *Rep.SAMSO-TR-78-24, ADA 061 324*, Air Force Sys. Command, Los Angeles, CA, 1978.
- Whipple, E.C., Potentials of surfaces in space, *Rep. Prog. Phys.*, Vol.44, 1197, 1981.

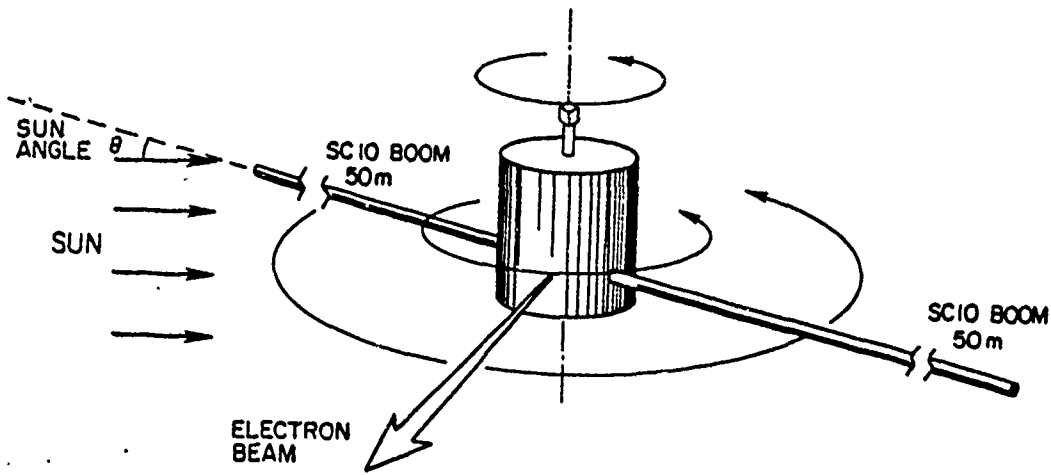


Figure 1. Schematic diagram of the SCATHA satellite with beam emission (from *Lai et al*, 1987).

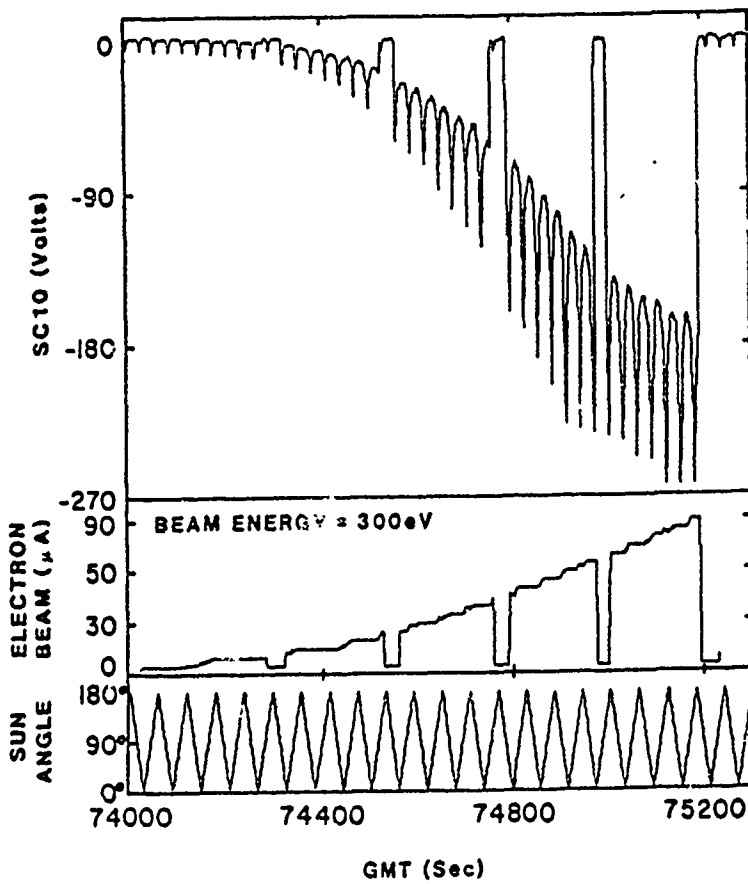


Figure 2. Day 70 SC10  $\phi$  data (Volts), electron beam current  $I_{beam}$  ( $\mu A$ ), and SC10 boom sun angle  $\theta$  (degrees) as functions of time. The electron beam energy is 300eV. The drop outs at regular intervals are for calibration.

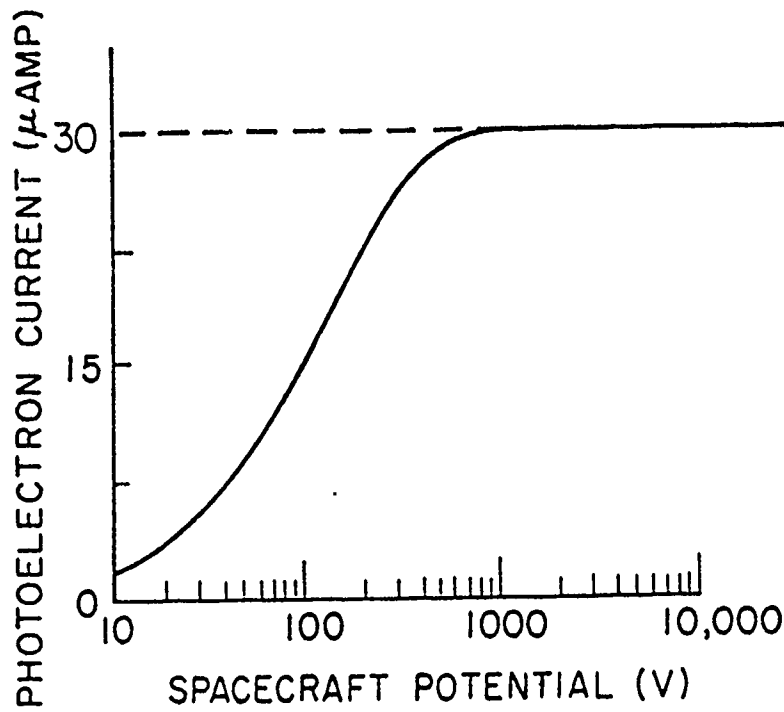


Figure 3. Total photoelectron current  $I_{pe}(\phi_s)$  arriving at the spacecraft body as a function of spacecraft potential  $\phi_s$ . The photoemissivity  $j_{ph}$  used is 3 nanoamp.cm<sup>-2</sup>.

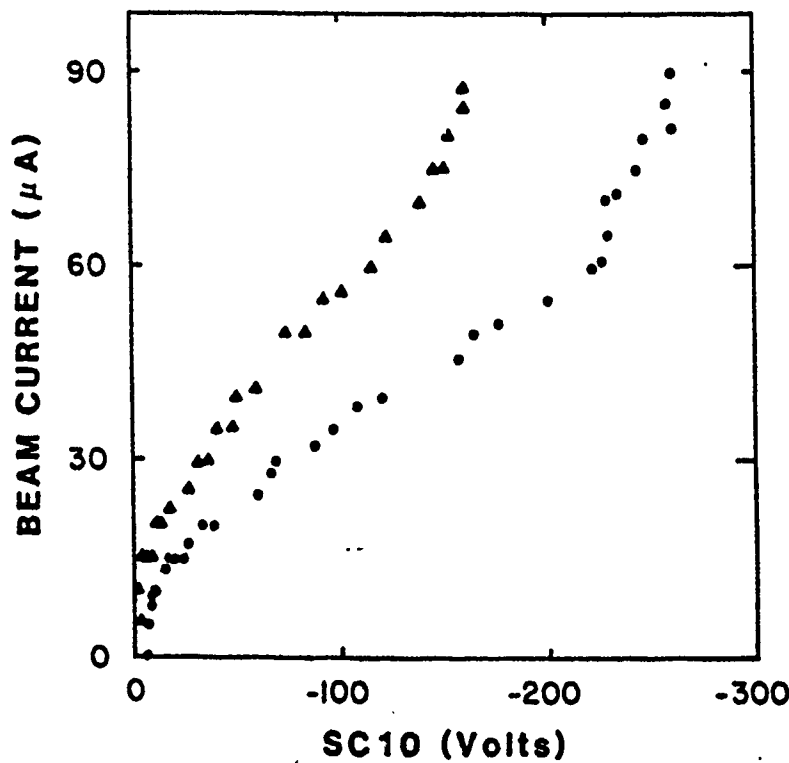


Figure 4. The maxima and minima of SC10 data (from Figure 2) as functions of emitted beam current.



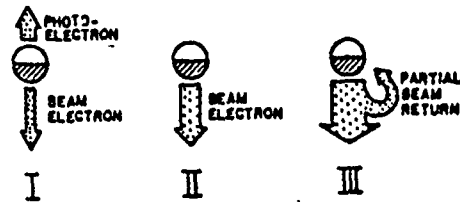
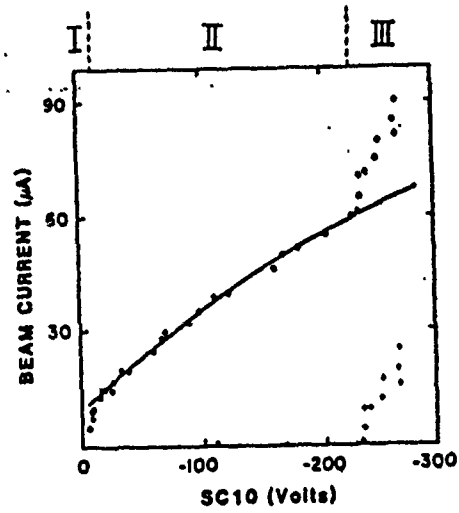


Figure 5. The emitted beam current  $I_{\text{beam}}$  and the SC10 data without photoemission (maximum  $|\phi|$  with  $\theta=0$  or  $180^\circ$ ). The three regimes are discussed in the text. The cartoons below the x-axis show schematically the physical processes in the regimes.

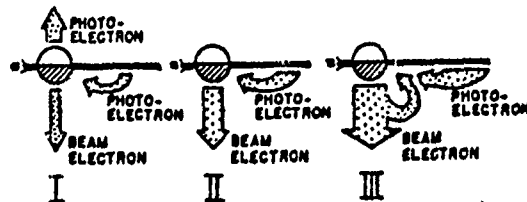
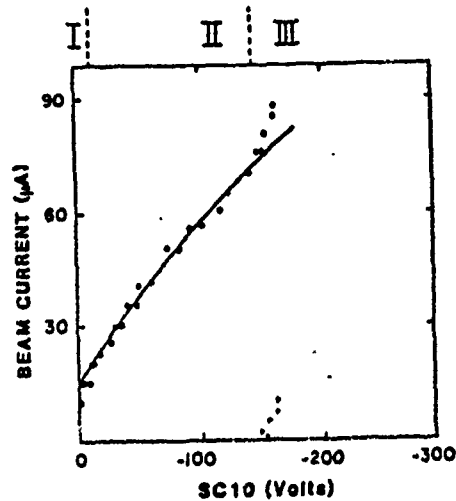


Figure 6. The emitted beam current  $I_{\text{beam}}$  and the SC10 data with photoemission (minimum  $|\phi|$  with  $\theta=90^\circ$  or  $270^\circ$ ). The three regimes are discussed in the text. The cartoons below the x-axis show schematically the physical processes in the regimes.

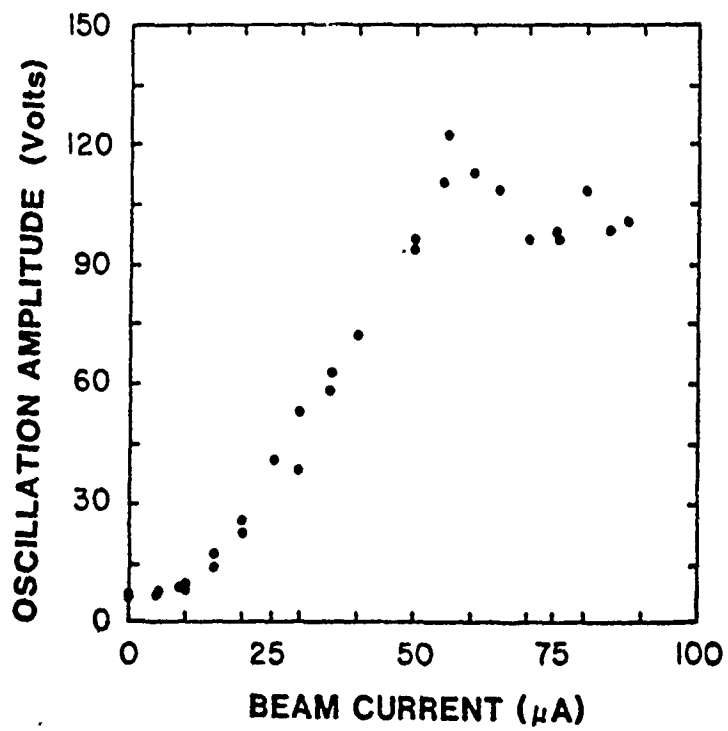


Figure 7. Non-monotonic behavior of the oscillation amplitude  $\Delta\phi$  of SC10 as a function of emitted beam current  $I_{\text{beam}}$ . Saturation occurs when the beam current exceeds a critical value.